

A Cooperative Oxygen Binding Hemoglobin from *Mycobacterium tuberculosis*

STABILIZATION OF HEME LIGANDS BY A DISTAL TYROSINE RESIDUE*

(Received for publication, September 15, 1999, and in revised form, October 20, 1999)

Syun-Ru Yeh^{‡§}, Manon Couture^{‡¶}, Yannick Ouellet[¶], Michel Guertin[¶], and Denis L. Rousseau[‡]

From the [‡]Department of Physiology and Biophysics, Albert Einstein College of Medicine, Bronx, New York 10461 and the [¶]Department of Biochemistry, Faculty of Sciences and Engineering, Laval University, Quebec, G1K 7P4, Canada

The homodimeric hemoglobin (HbN) from *Mycobacterium tuberculosis* displays an extremely high oxygen binding affinity and cooperativity. Sequence alignment with other hemoglobins suggests that the proximal F8 ligand is histidine, the distal E7 residue is leucine, and the B10 position is occupied by tyrosine. To determine how these heme pocket residues regulate the ligand binding affinities and physiological functions of HbN, we have measured the resonance Raman spectra of the O₂, CO, and OH⁻ derivatives of the wild type protein and the B10 Tyr → Leu and Phe mutants. Taken together these data demonstrate a unique distal environment in which the heme bound ligands strongly interact with the B10 tyrosine residue. The implications of these data on the physiological functions of HbN and another heme-containing protein, cytochrome *c* oxidase, are considered.

Invertebrate, plant, and bacterial hemoglobins have been the topic of many investigations in recent years in view of their peculiar physiological roles (1). The homodimeric hemoglobin from the aerobic bacterium, *Vitreoscilla*, is transcribed under oxygen-limiting growth conditions (2, 3). It is postulated that the protein acts as an oxygen carrier under hypoxic conditions and facilitates oxygen diffusion to the terminal oxidase complex. The hemoglobin in the eukaryotic green alga, *Chlamydomonas eugametos*, is expressed in response to activation of photosynthesis (4, 5). It is proposed to be involved with the photosynthetic electron transfer chains. The leghemoglobins discovered in plants function as oxygen scavengers, preventing the oxidation of the O₂-sensitive nitrogen-fixing machinery of the symbiotic *Rhizobium* bacteroids (6). In *Escherichia coli* and *Salmonella typhimurium*, a two-domain flavo-hemoglobin is involved in detoxification of nitric oxide (7–9). Despite this wide array of the physiological functions, all the hemoglobins discovered so far are made of myoglobin-like subunits with a three-over-three α -helical sandwich motif (globin fold) (1).

Recently, we expressed and characterized a hemoglobin (HbN)¹ from *Mycobacterium tuberculosis* that adds a new twist to the scope of the properties of invertebrate hemoglobins (10). HbN is a homodimeric protein. It displays extremely high oxygen binding affinity and cooperativity, with a Hill coefficient

of approximately 2. The sequence alignment with hemoglobins from alga, protozoa, and cyanobacteria suggests that the proximal ligand is His, the distal ligand at the E7 position is Leu, and that at the B10 position is Tyr. To examine the structure of the heme pocket and thereby infer the function of this hemoglobin, we have measured the resonance Raman spectra of the wild type protein and the Tyr → Leu and Tyr → Phe mutants under a variety of oxidation and ligand binding states. The resonance Raman spectra reveal distal features that are unique among the hemoglobins and demonstrate the essential role of B10 Tyr in stabilizing the heme-bound ligands.

EXPERIMENTAL PROCEDURES

Recombinant *M. tuberculosis* HbN was cloned, expressed, and purified to near homogeneity as described elsewhere (10). The single amino acid substitution mutants of HbN (Y33L and Y33F) were prepared as described previously (10). The protein was buffered at the desired pH with 50 mM Tris and CAPS at pH 7.5 and 10.5, respectively. For all of the experiments reported here, the protein concentration was 50 μ M. The Raman measurements were made with previously described instrumentation (11). The output at 406.7 nm from a krypton ion laser (Spectra Physics) was focused to an \sim 30 μ m spot (laser power \sim 2 mW) on a rotating cell to prevent photo-damage to the sample. The acquisition time was about 30 min for each spectrum. The scattered light was collected at right angles to the incident beam and focused on the entrance slit of a 1.25 m polychromator (Spex) where it was dispersed and then detected by a charge-coupled device camera (Princeton Instruments).

RESULTS

The general characteristics of resonance Raman spectra of heme proteins are well established (11, 12). In the high frequency region of the spectrum between 1300 and 1700 cm⁻¹, the oxidation state, spin state, and the axial coordination state of the iron at the center of the heme can be characterized. In particular, the ν_2 mode, in the region between 1550 and 1600 cm⁻¹, is sensitive to the iron spin state. The line in the 1475–1520 cm⁻¹ region, assigned as the ν_3 mode, is sensitive to both the axial coordination and spin state of the iron. The strong line between 1350 and 1400 cm⁻¹, assigned as the ν_4 mode, is sensitive to the π -electron density of the porphyrin macrocycle and, therefore, the oxidation state of the iron. The frequency and intensity of these Raman lines are further modulated by the protein environment surrounding the heme and, therefore, provide useful structural information on heme proteins. In the low frequency region of the spectrum between 200 and 800 cm⁻¹, the specific axial ligands coordinated to the prosthetic heme group can be identified by detecting iron-ligand stretching modes.

Ligand-free Ferrous HbN—The high frequency resonance Raman spectrum of the wild type ferrous deoxy form of HbN, shown in Fig. 1A, displays a typical five-coordinate high spin pattern with the electron density line (ν_4) appearing at 1356 cm⁻¹ and the strong spin/coordination sensitive line (ν_3) ap-

* The costs of publication of this article were defrayed in part by the payment of page charges. This article must therefore be hereby marked "advertisement" in accordance with 18 U.S.C. Section 1734 solely to indicate this fact.

§ To whom correspondence should be addressed. Tel.: (718) 430-4234; Fax: (718) 430-4230; E-mail: syeh@aecom.yu.edu.

¹ The abbreviations used are: HbN, homodimeric hemoglobin; CCP, cytochrome *c* peroxidase; HRP, horse radish peroxidase; CCO, cytochrome *c* oxidase; CAPS, 3-(cyclohexylamino)propanesulfonic acid.

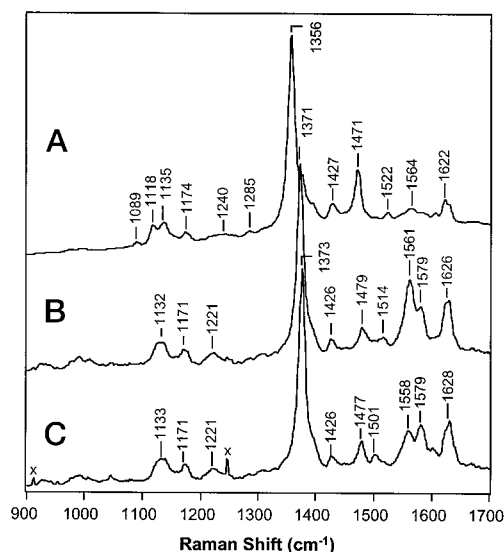


FIG. 1. The high frequency resonance Raman spectra of the wild type HbN. A, the ferrous protein at pH 7.5; B, the ferric protein at pH 7.5; C, the ferric protein at pH 10.5. The peaks indicated with \times are laser plasma lines.

pearing at 1471 cm^{-1} . In the low frequency region, shown in Fig. 2A, a strong line is detected at 226 cm^{-1} that is assigned as the iron-histidine (Fe-His) stretching mode. This confirms the prediction from the sequence alignment that histidine is the proximal ligand. The same spectra were obtained for the B10 Tyr \rightarrow Leu and Phe mutants (data not shown). The frequency of the Fe-His stretching mode is significantly higher than that in any other globin (Table I) and indicates that, unlike other cooperative hemoglobins, there is no proximal strain in this hemoglobin.

Ferric HbN—At neutral pH, the resonance Raman spectrum of the ferric protein is primarily six-coordinate and high spin as indicated by the 1479 and 1561 cm^{-1} lines for ν_3 and ν_2 , respectively (Fig. 1B). A contribution from a six-coordinate low spin form developed as the pH was raised from 7.5 to 10.5 as indicated by an increase in intensity of the lines at 1501 and 1579 cm^{-1} for ν_3 and ν_2 , respectively (Fig. 1C). This is consistent with the optical absorption spectra, in which the intensities of bands at 410 , 543 , and 578 nm increase with respect to those at 406 , 503 , and 624 nm as the pH is increased. With H_2^{16}O – H_2^{18}O isotopic substitution at pH 10.5, two isotope sensitive lines were detected at 454 and 561 cm^{-1} in H_2^{16}O , which shift to 423 and 533 cm^{-1} , respectively, in H_2^{18}O (Fig. 2D). Based on the isotope shifts, both of these lines are assigned as Fe–OH stretching modes. The resonance Raman spectra of the B10 Tyr \rightarrow Leu and Phe mutants of the ferric protein were also measured. In the B10 Tyr \rightarrow Phe mutant, the line at 454 cm^{-1} totally disappeared leaving only the high frequency line, which appeared at about 552 cm^{-1} in H_2^{16}O and shifted to 520 cm^{-1} in H_2^{18}O (Fig. 2E). Associated with this change in the Fe–OH stretching mode, in the high frequency region of the spectrum, the high spin marker line at 1479 cm^{-1} is diminished in comparison with the low spin marker line at 1501 cm^{-1} (data not shown). The Raman spectrum of the B10 Tyr \rightarrow Leu mutant is not detectable because of a high fluorescence background in this preparation (data not shown).

O_2 -bound Ferrous HbN—In the resonance Raman spectrum of the wild type ferrous oxy-derivative, one line was detected at 560 cm^{-1} that had oxygen isotope sensitivity (Fig. 3, A and C). In the difference spectrum, a positive peak at 563 cm^{-1} for $^{16}\text{O}_2$ is shifted to 542 cm^{-1} for $^{18}\text{O}_2$, in accord with the predicted shift for a Fe– O_2 diatomic oscillator of 23 cm^{-1} . As may be seen

by inspection of Table I, this mode is lower in HbN than in any other hemoglobin. In the B10 Tyr \rightarrow Leu mutant, the Fe– O_2 stretching mode is located at 570 cm^{-1} for $^{16}\text{O}_2$ and shifted to 545 cm^{-1} with $^{18}\text{O}_2$ (Fig. 3, B and D). In the mutant, the Fe– O_2 stretching mode has the same frequency as that observed in most other hemoglobins and myoglobins.

CO-bound Ferrous HbN—Unlike the oxy-derivative in which only a single Fe– O_2 stretching mode was present, two Fe–CO stretching modes at 534 and 500 cm^{-1} were detected in the spectrum of the $^{12}\text{C}^{16}\text{O}$ derivative of the ferrous protein (Fig. 4A) that shifted to 518 and 483 cm^{-1} in the $^{13}\text{C}^{18}\text{O}$ derivative (Fig. 4C). The relative intensity of these two modes is independent of pH, concentration of the protein, and incident laser power. In the resonance Raman spectra of the B10 Tyr \rightarrow Leu and Phe mutants, only one CO isotope sensitive line remained in the spectrum which was present at 500 cm^{-1} for the $^{12}\text{C}^{16}\text{O}$ derivative and at 489 cm^{-1} for the $^{13}\text{C}^{18}\text{O}$ derivative (Fig. 4, B and D).

In the C–O stretching region of the wild type spectrum, CO-isotope sensitive lines were also detected (Fig. 5). A strong line at 1916 cm^{-1} in $^{12}\text{C}^{16}\text{O}$ shifted to 1829 cm^{-1} in $^{13}\text{C}^{18}\text{O}$. Two lines centered at about 1960 cm^{-1} in $^{12}\text{C}^{16}\text{O}$ derivative appeared as only a single line at 1870 cm^{-1} in the $^{13}\text{C}^{18}\text{O}$ derivative. We assign the lines centered at 1960 cm^{-1} as originating from a Fermi resonance coupled pair involving a C–O stretching mode and a porphyrin mode. Upon the isotope substitution, this coupling is lost so only a single line appears in the $^{13}\text{C}^{18}\text{O}$ derivative. Based on these results, we assign the two Fe–CO stretching modes at 535 and 500 cm^{-1} as being associated with C–O stretching frequencies of 1916 and 1960 cm^{-1} , respectively.

DISCUSSION

Tyrosine Hydrogen Bonding—The frequencies of the various iron-ligand stretching modes of HbN reported here are compared with those of several other heme-containing proteins listed in Table I. It is evident from this table that the distal heme pocket of HbN is unique among the globins. When the B10 Tyr is mutated to either Leu or Phe, the iron-exogenous ligand modes convert to values similar to those of other globins, indicating that the B10 Tyr plays an important role in modulating the ligand binding properties of HbN. On the other hand, the Fe–His stretching frequency of HbN is not affected by the mutation at the B10 position, indicating that the changes in the distal environment do not propagate to the proximal side of the heme.

In vertebrate globins, the bound oxygen is stabilized by the distal histidine at the E7 position through hydrogen bonding to the terminal oxygen atom of O_2 as illustrated in Fig. 6 (13–15). The E7 residue in most invertebrate globins, on the other hand, is occupied by a glutamine (1). Stabilization of the ligand through the distal (E7) glutamine has been observed in *Lucina pectinata* and *Ascaris suum* hemoglobins (16). Intriguingly, the E7 Gln does not seem to play a crucial role in stabilizing the bound ligands in bacterial hemoglobins, apparently because of conformational constraints on this residue imposed by the polypeptide architecture. For example, the E7–10 region of the polypeptide in *Vitreoscilla*, instead of adopting the typical α -helical conformation, is disordered (17). As a result, the E7 Gln is rotated out of the heme pocket. Spectral and kinetic studies of the binding of oxygen and CO to E7 mutants of *Vitreoscilla* hemoglobin showed that this substitution had little effect on the ligand binding properties of this protein (18), evidence that E7 Gln does not hydrogen-bond to the bound ligand. The same segment in another bacterium, *Alcaligenes eutrophus*, adopts an elongated and well defined E-helix but deviates significantly from that in other globins by more than

FIG. 2. The low frequency resonance Raman spectra of the wild type HbN. A, the ferrous protein at pH 7.5; B, the ferric protein at pH 7.5; C, the ferric protein at pH 10.5. Traces D and E correspond to the difference spectrum between $H_2^{16}O$ and $H_2^{18}O$ at pH 10.5 for the wild type ferric protein and the B10 Tyr \rightarrow Phe mutant, respectively.

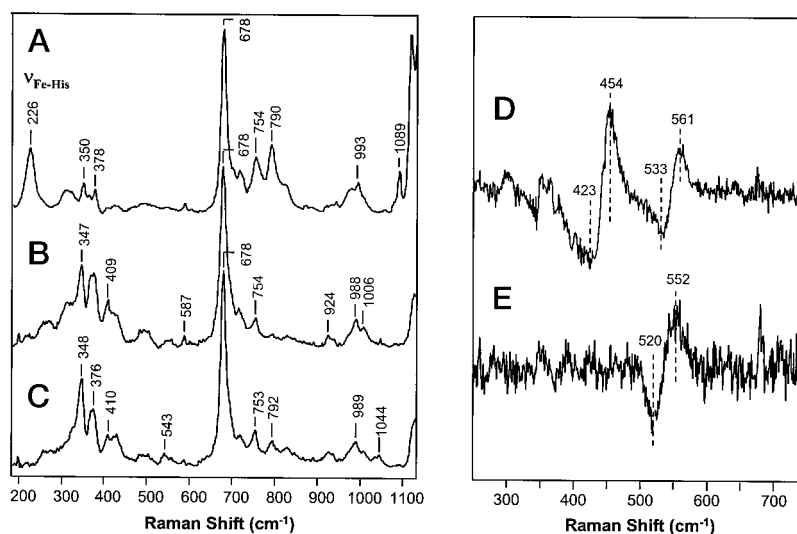


TABLE I

The frequencies of the iron-histidine ($Fe-His$), iron-hydroxide ($Fe-OH^-$), iron-CO ($Fe-CO$) and iron- O_2 ($Fe-O_2$) stretching modes of various heme-containing proteins determined by resonance Raman scattering. HS, LS, and 5C stand for high spin, low spin, and five-coordinated species, respectively; ND, not determined.

Proteins	ν_{Fe-His}	ν_{Fe-OH}	ν_{Fe-CO}	ν_{Fe-O_2}	References
HbN	226	454 (HS), 561 (LS)	500, 535	560	This work
HbN B10 mutants	226	552 (LS)	502	570	This work
Sperm Whale Mb	220	490 (HS), 551 (LS)	507	569	(30, 42, 43)
Human Hb	216	492 (HS), 553 (LS)	506	571	(30, 42, 43)
Scapharca Hb	203	578 (5C)	517	568	(42, 44)
<i>Ascaris suum</i> Hb	206	ND	515, 543	ND	(16, 50)
Barley Hb	219	ND	493, 534	ND	(45)
<i>Chlamydomonas</i> Hb	232	ND	491	ND	(46)
CCP	227, 248	ND	505, 537	ND	(47)
HRP	241, 244	492 (HS), 502 (LS)	531, 541	562	(30, 43, 47)
CCO	213	450, 477	494, 520	568	(29, 48, 49)

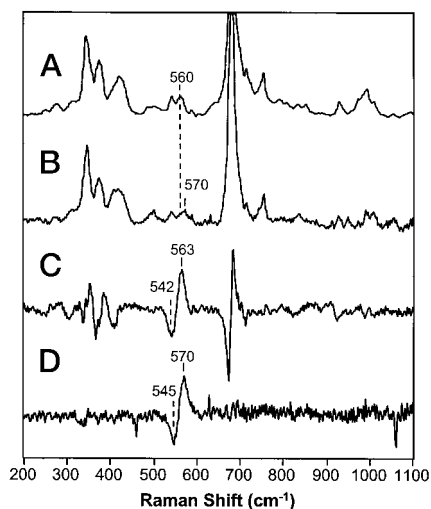


FIG. 3. The low frequency resonance Raman spectra of the ferrous O_2 -bound forms of HbN. A, wild type protein; B, the B10 Tyr \rightarrow Leu mutant at pH 7.5. Traces C and D correspond to the difference spectra between $^{16}O_2$ and $^{18}O_2$ for the wild type protein and the B10 Tyr \rightarrow Leu mutant, respectively.

10° because of an increase in the angle between E and F helices (19). This leads to a much more open distal pocket and causes a much larger entropic energy barrier for the E7 residue to interact with heme bound ligands.

Ligand stabilization in invertebrate and bacterial hemoglobins can also be achieved through a distal tyrosine at the B10 position (1, 17). When the hydroxyl group of the B10 Tyr is properly positioned in the heme distal site as in the Hb from

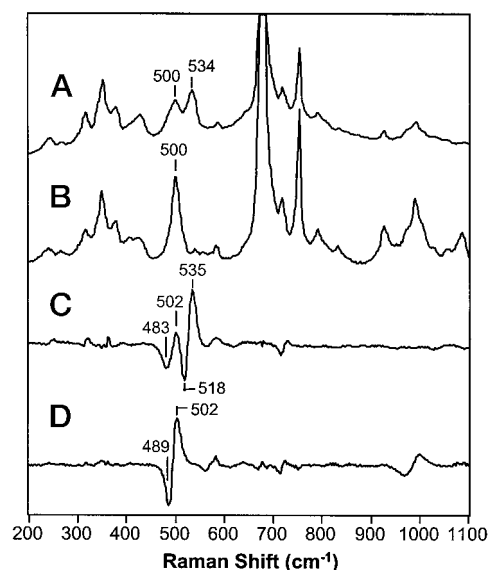


FIG. 4. The low frequency resonance Raman spectra of the ferrous CO-bound forms of HbN. A, the wild type protein; B, the B10 Tyr \rightarrow Leu mutant at pH 7.5. Traces C and D correspond to the difference spectra between $^{12}C^{16}O$ and $^{13}C^{18}O$ for the wild type protein and the B10 Tyr \rightarrow Leu mutant, respectively. In trace D, the signal at $\sim 1,000\text{ cm}^{-1}$ is assigned as the overtone of the Fe-CO stretching mode.

Ascaris (Fig. 6), very low ligand dissociation rates are observed (20). In contrast, the oxygen dissociation rate of a myoglobin mutant with the B10 Leu mutated to Tyr is increased because of the unfavorable B10 Tyr- O_2 contacts (20, 21).

In HbN, the E7 position is occupied by Leu. Thus, possible

FIG. 5. The high frequency resonance Raman spectra of the ferrous CO-bound forms of HbN at pH 7.5. Traces A and B correspond to $^{12}\text{C}^{16}\text{O}$ and $^{13}\text{C}^{18}\text{O}$, respectively. Trace C is the difference spectrum between traces A and B. Trace D, the correlation diagram of the Fe-CO stretching frequency and the C-O stretching frequency for a variety of heme proteins and porphyrin derivatives. The points for HbN (the filled circles) lie on the imidazole/histidine correlation line.

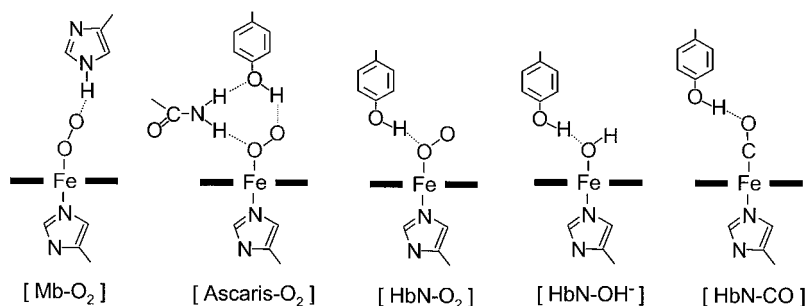
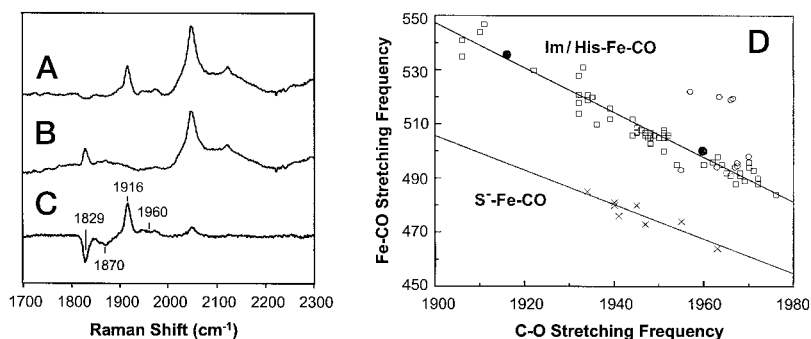


FIG. 6. The hydrogen bonding network for stabilizing the bound ligands in myoglobin (*Mb*), *A. suum* Hb, and HbN.

stabilization of heme-bound ligands by this residue is excluded. On the other hand, the role of the B10 residue in HbN on the stabilization of the bound oxygen is clear. The frequency of the Fe-O₂ stretching mode of HbN (560 cm⁻¹) is very low as compared with that in other globins in which the mode is located at approximately 570 cm⁻¹ (22). In general, as the O-O bond of the bound O₂ is highly polarized by the heme iron, the Fe-O₂ stretching frequency is relatively insensitive to distal residue mutations (22), but in HbN the frequency of the Fe-O₂ mode is very sensitive to the distal B10 mutation. We propose that the low frequency of the Fe-O₂ stretching mode in wild type HbN is the result of a unique hydrogen bonding pattern between the bound oxygen and the distal Tyr, as illustrated in Fig. 6, in which the bound oxygen is hydrogen-bonded to the distal Tyr through the *sp*² orbital of the proximal oxygen atom. This hydrogen bonding directly constrains and weakens the Fe-O₂ bond as indicated by the low Fe-O₂ stretching frequency. Mutation of the B10 Tyr to Leu or Phe releases the oxygen, and thus the frequency of the Fe-O₂ stretching mode shifts to 570 cm⁻¹, a frequency identical to that in the vertebrate globins.

A similar type of hydrogen bond has been found in *A. suum* Hb between a distal Gln and the bound oxygen based on crystallographic studies (23) as illustrated in Fig. 6, in which the bound oxygen is hydrogen-bonded to a distal glutamine and a tyrosine through the proximal and terminal oxygen atoms, respectively. Like HbN, two conformations of the CO-bound form were observed in *Ascaris* Hb. The Fe-CO stretching mode (543 cm⁻¹) in the closed conformation is higher than that of HbN. It has been postulated that the high frequency is a consequence of hydrogen bonding to the CO by both the Gln and the Tyr residues. Mutating B10 Tyr to Phe in *Ascaris* Hb causes the frequency to shift down to 520 cm⁻¹, reflecting the loss of the hydrogen bonding contribution from the Tyr (50).

In the CO-derivative of HbN, the B10 tyrosine mutation causes the disappearance of the line at 535 cm⁻¹, with only the 500 cm⁻¹ line remaining. Therefore, we assign the high frequency mode located at 535 cm⁻¹ as originating from a closed conformation in which the distal B10 Tyr strongly interacts with the CO as illustrated in Fig. 6 (conformational rearrangements may be required for the B10 Tyr to interact the oxygen

atom of the CO). This is a positive polar interaction which we attribute to hydrogen bonding with the proton on the tyrosine. It is well established that positive polar interactions weaken the C-O bond (lowering its stretching frequency) and strengthening the Fe-CO bond (increasing its stretching frequency) (24-26). The 500 cm⁻¹ band is assigned as an open conformation without this strong hydrogen bonding interaction. This latter frequency is similar to that reported in vertebrate globins.

Because of the electronic structure of the Fe-C-O moiety, when the distal interactions strengthen the C-O bond and concomitantly weaken the Fe-CO bond (or *vice versa*), there is an inverse correlation curve relating the frequencies of the Fe-CO stretching modes with those of the associated C-O stretching modes (27-29). These curves depend on the identity of the proximal ligand, such that the curve for imidazole/histidine is distinct from that of thiolate. Both of the CO-bound structures of HbN fall on the imidazole/histidine correlation curve as shown in Fig. 5D. This is consistent with the assignment of the proximal ligand as a histidine and the frequency difference between the two forms resulting from a hydrogen-bonding interaction between a distal residue and the CO. Furthermore, because the two data points fall on the same correlation curve, the presence of this hydrogen bond does not affect the His-Fe-CO σ -bonding system.

The presence of two conformations in the carbon monoxide derivative, in contrast to a single conformation for the oxy-derivative, is attributed to the difference in the intrinsic hydrogen bonding strength between tyrosine and the bound ligand as well as their relative orientation. The bound O₂ in the oxy-derivative may be optimally positioned for forming the hydrogen bond with the B10 Tyr as illustrated in Fig. 6. It is locked in the closed conformation because the tyrosine forms a very strong hydrogen bond with the O₂ such that the gain in enthalpy overcomes the loss in the conformational entropy. In contrast, the intrinsic hydrogen bonding strength between CO and Tyr is weaker, and the conformational entropy cost is high because of a preferred linear geometry of the bound CO and the location of the B10 Tyr in HbN which is optimized for forming a hydrogen bond with the proximal oxygen atom of the bound O₂ (Fig. 5). As a result, the gain in enthalpy is not enough to

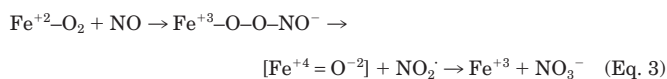
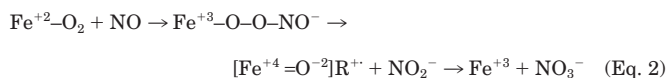
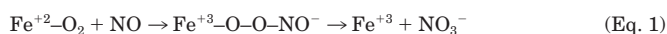
compensate for the loss in conformational entropy such that the carbon-monoxide derivative is in a thermal equilibrium between an open and a closed conformation.

Feis *et al.* (30) carried out an in-depth study of hydroxide modes in heme proteins. The Fe–OH stretching mode is found at 550 and 553 cm^{-1} in low spin metmyoglobin and methemoglobin, respectively, and at 491 and 492 cm^{-1} for the high spin forms of these proteins (Table I). The two hydroxy modes of HbN were identified at 456 and 560 cm^{-1} for the high and low spin forms, respectively. The observation that the Fe–OH stretching mode of the high spin species appears nearly 40 cm^{-1} lower than in other hemoglobins or myoglobins confirms the presence of the very strong hydrogen bond between the hydroxide moiety and the B10 Tyr. A similar shift is detected in the low spin form of horseradish peroxidase (30), in which the mode is detected at 503 cm^{-1} , 50 cm^{-1} lower than the low spin forms of the globins. This low frequency has also been attributed to very strong hydrogen bonding to the hydroxide in HRP.

The Physiological Function of HbN—In a previous report, we postulated that the physiological function of HbN is to protect the *M. tuberculosis* bacterium against attack by NO during its latent phase (10). Similar functions have been proposed for newly discovered flavohemoglobins in bacteria (7–9), suggesting that the detoxification of NO may be a more ancient function for the widely distributed hemoglobins (31). The structural features of HbN revealed by resonance Raman scattering are distinct from those of other globins. These properties demonstrate that the iron-bound ligands strongly interact with the tyrosine in the distal pocket. Such interactions are absent in normal oxygen storage and transport globins but are present in other heme-containing proteins that are involved in oxygen chemistry such as the peroxidases (32). These data thereby suggest that the unique heme pocket of HbN may be optimized for performing oxygen chemistry with NO.

It was demonstrated in vertebrate hemoglobin that the oxy-derivative reacts with NO and results in nitrate (33, 34). Recent kinetic studies suggest that this reaction goes through a peroxynitrite intermediate ($\text{Hb}^{+3}\text{-O-O-NO}^-$) as described in Equation 1.

Because the conversion from the peroxynitrite intermediate to nitrate and a ferric protein must involve O–O bond cleavage, the reaction is proposed to proceed through an oxy-ferryl ($\text{Fe}^{+4}=\text{O}$) intermediate as observed in the reaction between NO and model porphyrin compounds (35) and illustrated in Equation 2 or Equation 3.



In Equations 2 and 3, the reaction goes through a compound I, a heterolytic O–O bond cleavage product, and compound II, a homolytic O–O bond cleavage product, respectively (36, 37). Both the compound I and II species have been identified in the catalytic cycle of peroxidases. To generate compound I-like species, the iron needs to receive one electron from either the porphyrin or a nearby amino acid residue which is indicated as R^{+} in Equation 2. A good candidate for this amino acid residue in HbN is the B10 Tyr which may supply the redox equivalent needed for catalyzing the O–O bond heterolytic cleavage. More kinetic studies are required to confirm this model although the

oxy-ferryl species may not be observable if the O–O bond breakage is much slower than the subsequent reaction to NO_3^- .

Implications for Structure of the Binuclear Site in Cytochrome c Oxidase—The only other heme protein that has a frequency for its Fe–OH stretching mode as low as that reported here for HbN (454 cm^{-1}) is cytochrome *c* oxidase, in which the mode is detected at 450 cm^{-1} . No suitable explanation for the origin of this low frequency has been put forth. Cytochrome *c* oxidase catalyzes the reduction of oxygen to water through a complex series of intermediates. Recent crystallographic data have shown that one of the Cu_B ligands, His-240, is cross-linked to Tyr-244 at the heme $\text{a}_3\text{-Cu}_B$ catalytic site of the enzyme and that this cross-linked tyrosine is ideally positioned to participate in the dioxygen reduction (38). The experiments reported here give support to the proposal that the tyrosine in cytochrome *c* oxidase plays a critical role in interacting with the bound ligands. The similarity of the stretching frequencies of the Fe–OH stretching modes in these two proteins, which are significantly different from those in any other heme protein that have been reported, suggests that the two proteins have similar bonding motifs for the hydroxide derivatives. To test if this tyrosine modifies the functional and the spectroscopic properties of cytochrome *c* oxidase, site-directed mutagenesis studies have been reported. Unfortunately, the tyrosine plays such a critical role in stabilizing the structure of the protein that the mutants were nonfunctional and the catalytic site was completely disrupted (39). Thus, no conclusions could be drawn regarding the role of this residue from the mutagenesis experiments.

In some of the intermediates in cytochrome *c* oxidase, oxy-ferryl structures are formed. It has been proposed that a reducing equivalent for the formation of this intermediate can reside on the Tyr-244 (40). Support for this idea has come from EPR measurements in which a radical signal from a tyrosine residue was detected (41). Thus, it is quite possible that this radical is an intermediate in the mechanism of oxygen reduction. The putative tyrosine radical is thought to be re-reduced by the subsequent electron transfer events. A similar functional role for the B10 tyrosine of HbN is proposed here during the conversion of NO to nitrate as illustrated in Equation 2. In this case, the tyrosine radical intermediate is presumably re-reduced by the substrate, NO_2^- . It is interesting to consider that these very different proteins may exploit very similar mechanisms to carry out their reaction chemistry.

REFERENCES

- Bolognesi, M., Bordo, D., Rizzi, M., Tarricone, C., and Ascenzi, P. (1997) *Prog. Biophys. Mol. Biol.* **68**, 29–68
- Wakabayashi, S., Matsubara, H., and Webster, D. A. (1986) *Nature* **322**, 481–483
- Tsai, P. S., Kallio, P. T., and Bailey, J. E. (1995) *Biotechnol. Prog.* **11**, 288–293
- Couture, M., Chamberland, H., St-Pierre, B., Lafontaine, J., and Guertin, M. (1994) *Mol. Gen. Genet.* **243**, 185–197
- Couture, M., and Guertin, M. (1996) *Eur. J. Biochem.* **242**, 779–787
- Appleby, C. A. (1984) *Annu. Rev. Plant Physiol.* **35**, 443–478
- Crawford, M. J., and Goldberg, D. E. (1998) *J. Biol. Chem.* **273**, 12543–12547
- Kim, S. O., Orii, Y., Lloyd, D., Hughes, M. N., and Poole, R. K. (1999) *FEBS Lett.* **445**, 389–394
- Cramm, R., Siddiqui, R. A., and Friedrich, B. (1994) *J. Biol. Chem.* **269**, 7349–7354
- Couture, M., Yeh, S.-R., Wittenberg, B. A., Wittenberg, J. B., Ouellet, Y., Rousseau, D. L., and Guertin, M. (1999) *Proc. Natl. Acad. Sci. U. S. A.* **96**, 11223–11228
- Wang, J., Caughey, W. S., and Rousseau, D. L. (1996) in *Methods in Nitric Oxide Research* (Feelisch, M., and Stamlie, J. S., eds), pp. 427–454, John Wiley & Sons Inc., New York
- Hu, S., Smith, K. M., Frei, H., and Spiro, T. G. (1996) *J. Am. Chem. Soc.* **118**, 12638–12646
- Phillips, S. E., and Schoenborn, B. P. (1981) *Nature* **292**, 81–82
- Olson, J. S., and Phillips, G. N., Jr. (1996) *J. Biol. Chem.* **271**, 17593–17596
- Kitagawa, T., Ondrias, M. R., Rousseau, D. L., Ikeda-Saito, M., and Yonetani, T. (1982) *Nature* **298**, 869–871
- Peterson, E. S., Huang, S., Wang, J., Miller, L. M., Vidugiris, G., Kloek, A. P., Goldberg, D. E., Chance, M. R., Wittenberg, J. B., and Friedman, J. M.

- (1997) *Biochemistry* **36**, 13110–13121
17. Tarricone, C., Galizzi, A., Coda, A., Ascenzi, P., and Bolognesi, M. (1997) *Structure* **5**, 497–507
 18. Dikshit, K. L., Orii, Y., Navani, N., Patel, S., Huang, H. Y., Stark, B. C., and Webster, D. A. (1998) *Arch. Biochem. Biophys.* **349**, 161–166
 19. Ermiler, U., Siddiqui, R. A., Cramm, R., and Friedrich, B. (1995) *EMBO J.* **14**, 6067–6077
 20. Gibson, Q. H., Regan, R., Olson, J. S., Carver, T. E., Dixon, B., Pohajdak, B., Sharma, P. K., and Vinogradov, S. N. (1993) *J. Biol. Chem.* **268**, 16993–16998
 21. Springer, B. A., Egeberg, K. D., Sligar, S. G., Rohlf, R. J., Mathews, A. J., and Olson, J. S. (1989) *J. Biol. Chem.* **264**, 3057–3060
 22. Hirota, S., Li, T., Phillips, G. N., Jr., Olson, J. S., Mukai, M., and Kitagawa, T. (1996) *J. Am. Chem. Soc.* **118**, 7845–7846
 23. Yang, J., Kloek, A. P., Goldberg, D. E., and Mathews, F. S. (1995) *Proc. Natl. Acad. Sci. U. S. A.* **92**, 4224–4228
 24. Li, T., Quillin, M. L., Phillips, G. N., Jr., and Olson, J. S. (1994) *Biochemistry* **33**, 1433–1446
 25. Kushkuley, B., and Stavrov, S. S. (1996) *Biophys. J.* **70**, 1214–1229
 26. Unno, M., Christian, J. F., Olson, J. S., Sage, J. T., and Champion, P. M. (1998) *J. Am. Chem. Soc.* **120**, 2670–2671
 27. Yu, N. T., Kerr, E. A., Ward, B., and Chang, C. K. (1983) *Biochemistry* **22**, 4534–4540
 28. Smulevich, G., Mauro, J. M., Fishel, L. A., English, A. M., Kraut, J., and Spiro, T. G. (1988) *Biochemistry* **27**, 5486–5492
 29. Rousseau, D. L., Ching, Y., and Wang, J. (1993) *J. Bioenerg. Biomembr.* **25**, 165–176
 30. Feis, A., Marzocchi, M. P., Paoli, M., and Smulevich, G. (1994) *Biochemistry* **33**, 4577–4583
 31. Zhu, H., and Riggs, A. F. (1992) *Proc. Natl. Acad. Sci. U. S. A.* **89**, 5015–5019
 32. Dawson, J. H. (1988) *Science* **240**, 433–439
 33. Herold, S. (1998) *FEBS Lett.* **439**, 85–88
 34. Eich, R. F., Li, T., Lemon, D. D., Doherty, D. H., Curry, S. R., Aitken, J. F., Mathews, A. J., Johnson, K. A., Smith, R. D., Phillips, G. N., Jr., and Olson, J. S. (1996) *Biochemistry* **35**, 6976–6983
 35. Lee, J., Hunt, J. A., and Groves, J. T. (1998) *J. Am. Chem. Soc.* **120**, 7493–7501
 36. Anni, H., and Yonetani, T. (1992) in *Metal Ions in Biological Systems* (Sigel, H., and Sigel, A., eds), Vol. 28, pp. 219–241, Marcel Dekker, Inc., New York
 37. Patterson, W. R., Poulos, T. L., and Goodin, D. B. (1995) *Biochemistry* **34**, 4342–4345
 38. Yoshikawa, S., Shinzawa-Itoh, K., Nakashima, R., Yaono, R., Yamashita, E., Inoue, N., Yao, M., Fei, M. J., Libeu, C. P., Mizushima, T., Yamaguchi, H., Tomizaki, T., and Tsukihara, T. (1998) *Science* **280**, 1723–1729
 39. Das, T. K., Pecoraro, C., Tomson, F. L., Gennis, R. B., and Rousseau, D. L. (1998) *Biochemistry* **37**, 14471–14476
 40. Proshlyakov, D. A., Pressler, M. A., and Babcock, G. T. (1998) *Proc. Natl. Acad. Sci. U. S. A.* **95**, 8020–8025
 41. MacMillan, F., Kannt, A., Behr, J., Prisner, T., and Michel, H. (1999) *Biochemistry* **38**, 9179–9184
 42. Song, S., Boffi, A., Chiancone, E., and Rousseau, D. L. (1993) *Biochemistry* **32**, 6330–6336
 43. Van Wart, H. E., and Zimmer, J. (1985) *J. Biol. Chem.* **260**, 8372–8377
 44. Das, T. K., Boffi, A., Chiancone, E., and Rousseau, D. L. (1999) *J. Biol. Chem.* **274**, 2916–2919
 45. Das, T. K., Lee, H. C., Duff, S. M., Hill, R. D., Peisach, J., Rousseau, D. L., Wittenberg, B. A., and Wittenberg, J. B. (1999) *J. Biol. Chem.* **274**, 4207–4212
 46. Couture, M., Das, T. K., Lee, H. C., Peisach, J., Rousseau, D. L., Wittenberg, B. A., Wittenberg, J. B., and Guertin, M. (1999) *J. Biol. Chem.* **274**, 6898–6910
 47. Dasgupta, S., Rousseau, D. L., Anni, H., and Yonetani, T. (1989) *J. Biol. Chem.* **264**, 654–662
 48. Han, S., Ching, Y. C., and Rousseau, D. L. (1990) *Nature* **348**, 89–90
 49. Sassaroli, M., Ching, Y. C., Argade, P. V., and Rousseau, D. L. (1988) *Biochemistry* **27**, 2496–2502
 50. Das, T. K., Friedman, J. M., Kloek, A. P., Goldberg, D. E., and Rousseau, D. L. (2000) *Biochemistry*, in press